

Interference Effects in the Auger Decay of the Resonantly Excited $2p_{3/2}^{-1}3d$ State of Argon

R. Camilloni¹ and M. Žitnik^{1,2}

¹*Istituto Metodologie Avanzate Inorganiche CNR, CP 10, 00016 Monterotondo, Italy*

²*"J. Stefan" Institute, University of Ljubljana, Jamova 39, 61000 Ljubljana, Slovenia*

C. Comicioli, K. C. Prince, and M. Zacchigna

Sincrotrone Trieste, Padriciano 99, 34012 Trieste, Italy

C. Crotti, C. Ottaviani, C. Quaresima, and P. Perfetti

Istituto di Struttura della Materia CNR, Via E. Fermi 38, 00044 Frascati, Italy

G. Stefani

Dip. di Fisica, Università di Roma Tre and INFN, P. le A. Moro 2, 00185 Roma, Italy

(Received 22 March 1996)

High resolution resonant Auger spectra have been measured at the VUV beam line at ELETTRA, Sincrotrone Trieste, while tuning the photon energy across the $2p_{3/2}^{-1}3d$ resonance of argon. A large variation of the branching ratio for decay into the spectator $3p^{-2}3d$ and shakeup $3p^{-2}4d$ channels is observed. The effect has not been seen previously in resonant inner-shell excitation and is attributed to the interference between the direct photoionization process and resonant Auger decay leading to the same final state. [S0031-9007(96)01195-7]

PACS numbers: 32.80.Hd, 32.80.Fb

When the excitation energy is below the threshold an inner-shell electron can only be promoted to one of the empty atomic levels. The relaxation usually proceeds via the resonant Auger process in which one of the outer electrons fills a core hole and another is ejected into the continuum. When the bandwidth of excitation energy is narrow compared to the natural width of the resonance the so-called Auger resonant Raman effect appears. Using well monochromatized synchrotron light as a probe, the energies of Auger peaks were seen to follow the photon energy across the inner shell resonances of Kr and Xe [1]. In addition, subnatural Auger linewidths were recorded, reflecting experimental resolution rather than natural width of the resonance. Both observations are analogous to the resonant Raman effect observed previously in inelastic x-ray scattering [2] and can be understood as a consequence of energy conservation. An as yet unanswered question relating directly to the validity of the two-step model is whether the intensity profiles of the resonant Auger lines follow the corresponding absorption resonance curve. The present Letter demonstrates that individual Auger intensity profiles may differ from the total absorption intensity profile. In fact, decay branching ratios may change drastically when going through the resonance as observed in the case of the $2p_{3/2}^{-1}3d$ resonance in argon.

We performed a series of high resolution resonant Auger measurements to study the lowest $2p^{-1}nl$ resonances in argon up to $2p_{3/2}^{-1}5d$ lying just 0.6 eV below the $2p_{3/2}$ ionization threshold at 248.63 eV [3]. Here we concentrate on the $2p_{3/2}^{-1}3d$ state having an excitation energy of 246.93 eV. The Auger decay pertaining to this particu-

lar resonance was observed previously [4–6] but no attempt was made to record the Auger line intensities versus the photon energy. Our measurements were carried out on the recently commissioned vacuum-ultraviolet (VUV) beam line at Sincrotrone Trieste [7]. The spherical grating monochromator is capable of a photon energy resolution at the Ar $2p$ threshold of 19 meV, but for the present experiment the slits were opened to provide higher flux. The analyzer is a 150 mm spherical deflection electron energy analyzer (VSW Ltd.) with a nominal $\pm 8^\circ$ of acceptance equipped with a 16 channel detector. The total experimental resolution was 112 meV as measured on the Ar $3s$ photoemission line. The photon bandwidth was determined from deconvolution of $2p_{1/2}^{-1}4s$ and $2p_{3/2}^{-1}3d$ absorption spectra taken just prior to the resonant Auger measurements. The analysis gave an 80 meV wide Gaussian component attributed to the photons and a 115 meV wide Lorentz profile which agrees well with a 118 ± 4 meV natural linewidth of $2p_{3/2}^{-1}3d$ resonance as given before [8].

A series of Auger spectra was measured in the kinetic energy range from 204 to 210 eV where the most intense *LMM* resonant Auger lines due to the decay of the $2p_{3/2}^{-1}3d$ resonance are found. Each of the spectra was recorded at different photon energy in order to cover the energy region of the resonance. The peak energies were seen to shift in step with the photon energy demonstrating again the Auger resonant Raman effect. The lines may be approximately assigned [9] as $3p^{-2}3d$ and $3p^{-2}4d$ states of Ar^+ , which are final states of the spectator and shakeup decay of the $2p_{3/2}^{-1}3d$ resonance, respectively. When the first resonant Auger spectrum in

TABLE I. Binding energies E_{bin} and assignment of some final states found in decay of the resonantly excited $2p_{1/2}^{-1}4s$ and $2p_{3/2}^{-1}3d$, $5s$ states of argon (Fig. 1). The strongest three eigenstate components are reported with weights corresponding to the absolute squares of mixing coefficients when the largest one is smaller than 90%. For brevity $3p^{-2}$ was omitted from labels everywhere except for $3s^{-1}$ configuration.

Peak	E_{bin}^a (eV)	Labels ^a	Labels ^b
0	29.24	$3s^{-1}2S$	$0.6\ 3s^{-1}2S/0.4(1D)3d^2S$
1	36.02	$(1D)3d^2F$	Same
2	36.50	$(1S)4s^2S$	Same
3	37.15	$(1D)3d^2D$	$0.3(3P)4d^2D/0.2(1D)3d^2D/0.2(3P)3d^2D$
4	37.40	$(1D)3d^2P$	$0.3(1D)3d^2P/0.3(3P)4d^2P/0.2(3P)3d^2P$
5	38.05	$(1S)3d^2D$	$0.6(1S)3d^2D/0.2(1D)3d^2D$
6	38.33	$(3P)5s^4P$	$(3P)5s^4.2P$
	38.49	$(3P)5s^2P$	$(3P)5s^4.2P$
	38.58	$(1D)3d^2S$	$0.5(1D)4d^2S/0.3(1D)3d^2S/0.1\ 3s^{-1}2S$
7	38.77	$(3P)4d^4F$	Same
8	39.36	$(3P)4d^2P$	$0.3(3P)4d^2P/0.2(1D)4d^2/0.1(1D)3d^2P$
9	39.64	$(3P)4d^2D$	$0.4(3P)5d^2D/0.2(3P)4d^2D/0.2(1S)3d^2D$
10	40.04	$(1D)5s^2D$	Same
11	40.38	$(1D)4d^2G$	Same
	40.50	$(1D)4d^2P$	$0.6(1D)4d^2D/0.1(3P)5d^4F/0.1(3P)5d^4D$
	40.53	$(1D)4d^2D$	$(1D)4d^2F$
12	41.21	$(1D)4d^2S$	$0.6(1D)5d^2S/0.3(1D)4d^2S/0.1\ 3s^{-1}2S$

^aSee Ref. [9]. E_{bin}^a is the average multiplet energy.

^bThis work.

argon was taken an anomalously strong shakeup process was observed [4]. An explanation was given within the framework of the sudden approximation, since calculations indicated large overlap integrals between the initial $3d$ atomic and relaxed ionic orbitals of the Rydberg electron. As the energy resolution was improved more details were found in the spectra [6] more or less in agreement with the assignments and decay probabilities obtained by restricted configuration interaction (CI) calculations in the Hartree-Fock (HF) model [5]. We performed extended CI calculations by running a Dirac-Fock multiconfigurational code [10] to optimize final ionic states including $3p^{-2}ns$, $3p^{-2}md$ configurations ($n = 4, 5$ and $m = 3-7$) together with $3s^{-1}$ which is well known [11] to mix with $3p^{-2}md$. The results confirm the strong parent mixing [5] and, in addition, they indicate that $3p^{-2}md$ configurations very strongly mix between themselves (Table I).

Some of the measured spectra are presented in Fig. 1. In order to allow for a direct comparison of the final state intensities at different photon energies, the Auger spectra were transformed into binding energy spectra by subtracting the photon energy. Counts are normalized to the same photon flux and target density. There are roughly five groups of peaks showing different intensity variation with respect to the photon energy. In the first group are peaks labeled 1, 7, 8, 9, and 12 which vanish equally fast on both sides of the resonance. The second group contains only peak 11 which becomes the dominant feature in spectrum 1(d) taken on the high energy side of the resonance. The third group of peaks, labeled 3,

4, and 5, becomes relatively strong on the low energy side of the resonance compared to members of the first and second groups. In spectrum 1(a) taken on the top

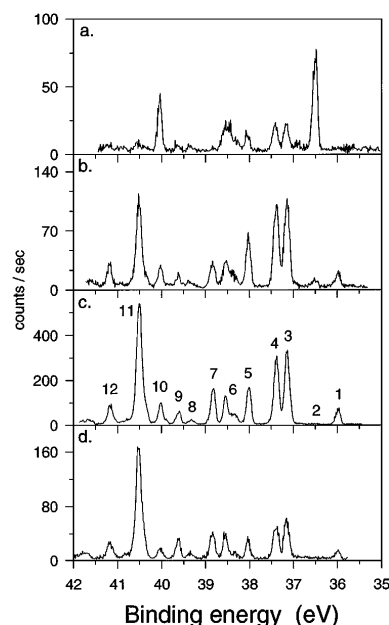


FIG. 1. Binding energy spectra from the resonant Auger spectra measured at photon energies: (a) 246.51 eV, on top of the $2p_{1/2}^{-1}4s$ resonance, (b) 246.80 eV, below the $2p_{3/2}^{-1}3d$ resonance, (c) 246.93 eV, on top of the $2p_{3/2}^{-1}3d$ resonance, and (d) 247.06 eV, above the $2p_{3/2}^{-1}3d$ resonance. In (c) the most prominent peaks are denoted by numbers; see Table I.

of the $2p_{1/2}^{-1}4s$ resonance 420 meV below the $2p_{3/2}^{-1}3d$ maximum, peaks 3, 4, and 5 are still clearly visible. In the fourth group there is peak 2 which belongs to the $3p^{-2}4s^2S$ final ionic state. The most intense, due to spectator decay of the $2p_{1/2}^{-1}4s$ resonance, is shown in Fig. 1(a) and vanishes at higher photon energies. Finally, peaks 6 and 10 are from group five, representing $3p^{-2}5s$ ionic states. They arise under both resonances, $2p_{1/2}^{-1}4s$ and $2p_{3/2}^{-1}3d$, indicating different decay paths. The first one is shakeup from the $3p^{-2}4s$ state while the second is spectator decay from $2p_{3/2}^{-1}5s$ hidden under the much stronger $2p_{3/2}^{-1}3d$ resonance.

In the two-step model the final state intensities are expected to change according to the probability for creating the resonance state which is given by the Breit-Wigner formula. The decay branching ratios are not expected to change. Figure 2(b) displays two constant ionic state (CIS) spectra derived from the resonant Auger spectra: each represents one group of final state with the most anomalous intensity profiles, namely the second group (peak 11) and the third group represented by the summed intensity of peak 3 and 4. Their intensity ratio was observed to change by an order of magnitude [Fig. 2(c)]. In previous experiments [5,6] the average value of the ratio over the resonance was determined to be close to 1 which agrees with our result but only when the photon energy E is close to E_r , the resonance energy.

Since the analyzer was positioned to be nearly at the magic angle with respect to the polarization axis of the light, even large differences in the asymmetry parameter behavior across the resonance could not change the intensity ratio as much as observed. It is also unlikely that variation of the ratio is due to the presence of multiple resonances overlapping closely in that energy range. One of them is $2p_{1/2}^{-1}5s^1P$ which was calculated to be 20 times weaker than the strongest $2p_{3/2}^{-1}3d^1P$, in agreement with the old result [14]. In addition, our final state configuration interaction (FISCI) calculations indicate that the probability for states 3, 4, and 11 to contain $3p^{-2}ns$ configurations ($n = 4, 5$) is smaller than 1%. All of this amounts to a negligible probability for the resonance $2p_{3/2}^{-1}5s^1P$ to decay into final states 3, 4, and 11. Another possible intermediate state is $2p_{3/2}^{-1}3d^3P$ and is again calculated to be 15 times weaker than the $2p_{3/2}^{-1}3d^1P$. Since they both decay to $3p^{-2}md$ states with comparable intensity [5] it is supposed that a major part of the resonant Auger intensity comes from decay of $2p_{3/2}^{-1}3d^1P$. Finally, decay paths from the neighboring $2p_{3/2}^{-1}4d$ resonance which is 740 meV away, are still not important on the high energy side of the $2p_{3/2}^{-1}3d$ resonance. The remaining possibility to be considered is the interference between the resonant process and a direct process leading to the same final state. This would give Fano-like CIS spectra with different shapes reflecting different relative strength of the two processes and possibly a large variation of intensity

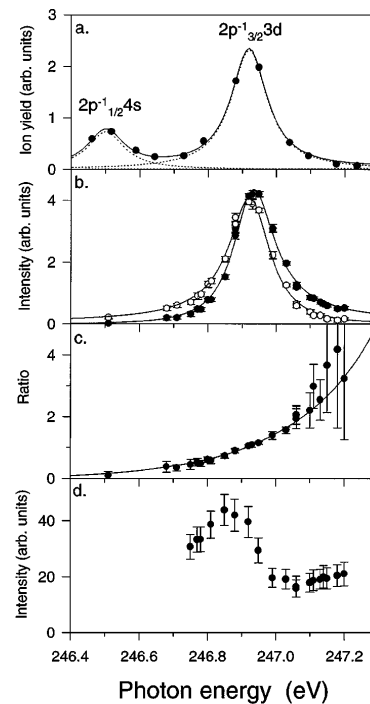


FIG. 2. (a) Photoabsorption spectrum in the region of $2p_{1/2}^{-1}4s$ and $2p_{3/2}^{-1}3d$, $5s$ resonances in Ar. Filled circles: measured points; full line: least-squares fit to the data. (b) CIS spectra for peak 11 (filled circles) and peak 3 + 4 (open circles). Full lines: least-squares fits of Fano profiles to the data; their ratio is given in (c) as a full line. (c) Ratio of intensity of peak 11 versus peak 3 + 4. Filled circles: experimental values. (d) CIS spectrum for the $3s^{-1}$ state.

ratio as a function of photon energy. The cross section for transition into the selected final state f in vicinity of the resonance may be written [13]

$$\sigma_f(E) = \sigma_0^f \frac{(E - E_r + q_f \Gamma/2)^2}{(E - E_r)^2 + \Gamma^2/4}, \quad (1)$$

where Γ is the total decay width of the resonance and σ_0^f is the cross section for direct excitation of the final ionic state. The line shapes depend on the value of the Fano parameter q_f and they approach the Lorentz form when σ_0^f goes to zero. The parametric form (1) was fitted to the two sets of experimental points, Fig. 2(b). The best fits gave the same values of parameters Γ , E_r , σ_0^f and the opposite values of parameter q_f of the two spectra. The probability for the direct process was estimated from the fit to be $(5 \pm 2) \times 10^{-3}$ of the maximum strength for the resonant process leading to final state 11. This corresponds to $(8 \pm 3)\%$ of intensity of the $3s$ photoemission line as determined from our measurements.

The $3p^{-2}md\epsilon l$ states can be reached directly from the ground state by absorption of one photon either in the so-called conjugate shakeup process [14] or with a dipolar transition from the ground state due to initial state configuration interaction (ISCI). The amplitude of the

conjugate shakeup process, as it involves interaction of photoelectron with valence electrons, decreases rapidly above the $3s^{-1}$ ionization threshold and is negligible in our energy range. To check for the latter we performed restricted ISCI calculations including $3p^{-2}md^2$ states up to $m = 8$. In the ground state of argon, a 1.6% admixture of these states was found and almost all of it (94%) is attributed to $3p^{-2}3d^2$ configuration. We calculated the dipole-length transition probabilities in the single electron HF approximation for continuum waves p, f of energy $\epsilon = 210$ eV in the final ionic state potential. Combining the results with ISCI weights the relative intensities of satellite lines at the magic angle are expected to be in the ratio $1:0.25:4 \times 10^{-5}$ for $m = 3, 4, 5$. Indeed, besides the series of $3p^{-2}(^1D)md, ns^2S$ satellite states due to the FISCI, also ISCI satellites were observed [15,16]. Two satellite peaks corresponding to peaks 3 and 4 are reported in Ref. [16], with an overall intensity of about 14% relative to the $3s$ photoemission line at a photon energy of 112.9 eV that agrees with the calculated cross sections [17]. This is not in contrast with the ratio obtained from our CIS spectrum with the fitting procedure. The satellites corresponding to peak 11 are also reported in Refs. [16,17]. The relative intensity is calculated to be less than 1% already at 120 eV [18]. The value $(8 \pm 3)\%$ deduced in our case from the fit appears to be too high. It has to be kept in mind that formula (1) applies in the case of interference of one resonant and one direct channel. A model that includes the other resonances, mainly the $2p_{3/2}^{-1}4d^1P$, would certainly be more appropriate. To obtain estimates for the direct process intensities leading to final states 3, 4, and 11, accurate measurements of the $3s$ satellite spectrum are needed at photon energies just below the $2p^{-1}ns, md$ resonances.

In Fig. 2(d) the CIS spectrum of the $3s$ photoemission line is presented and shows a Fano-like shape in the $2p_{3/2}^{-1}3d$ resonance region. This interference pattern has been seen before, although with an 8 times larger photon bandwidth [18]. Now, besides the direct photoionization from the ground state, the $3s^{-1}\epsilon l$ state can be reached via resonant decay into the $3p^{-2}3d$ component of the state (Table I). No $3s$ interference pattern was observed under the $2p_{3/2}^{-1}4s$ resonance.

A conclusion which can be drawn from these results is that if the resonant photoabsorption is measured by monitoring different decay channels, the intensity profiles may deviate from the Lorentzian form as well as from each other, due to their coupling to nonresonant channels. Strictly speaking, also the total absorption curve is then not a Lorentzian but the sum of Fano-like shapes. In the present case, however, a Lorentzian is a good approximation since the intensity profiles of the strongest two decay channels of the $2p_{3/2}^{-1}3d$ resonance are distorted in such a way to compensate in the total ion yield. To better under-

stand these results a coherent treatment of all three steps, excitation, decay and the shake process would be necessary.

Finally, we have studied the Auger resonant decay of the $2p_{3/2}^{-1}3d$ resonance of Ar at very high energy resolution of the photon beam. The branching ratio for the strongest Auger decay channels was observed to change drastically across the resonance. This is a new aspect of the Auger resonant Raman effect and is attributed to the interference between direct and resonant photoemission.

We acknowledge the excellent technical support of L. Romanzin and A. Rinaldi as well as the assistance of M. Štuhec in the course of computations.

-
- [1] A. Kivimäki, A. Naves de Brito, S. Aksela, O.-P. Sairanen, A. Ausmees, S.J. Osborne, L.B. Dantas, and S. Svensson, *Phys. Rev. Lett.* **71**, 4307 (1993).
 - [2] P. Eisenberger, P.M. Platzman, and H. Winick, *Phys. Rev. Lett.* **36**, 623 (1976).
 - [3] G.C. King, M. Tronc, F.H. Read, and R.C. Bradford, *J. Phys. B* **10**, 2479 (1977).
 - [4] H. Aksela, S. Aksela, H. Pulkkinen, G.M. Bancroft, and K.H. Tan, *Phys. Rev. A* **37**, 1798 (1988).
 - [5] M. Meyer, E.V. Raven, B. Sonntag, and J.E. Hansen, *Phys. Rev. A* **43**, 177 (1991).
 - [6] A. de Gouw, J. van Eck, A.C. Peters, J. van der Weg, and H.G.M. Heideman, *J. Phys. B* **28**, 2127 (1995).
 - [7] C. Quaresima, C. Ottaviani, M. Matteucci, C. Crotti, A. Antonini, M. Capozzi, S. Rinaldi, M. Luce, P. Perfetti, K.C. Prince, C. Astaldi, M. Zaccagna, L. Romanzin, and A. Savoia, *Nucl. Instrum. Methods Phys. Res., Sect. A* **364**, 374 (1995).
 - [8] D.A. Shaw, G.C. King, F.H. Read, and D. Cvejanović, *J. Phys. B* **15**, 1785 (1982).
 - [9] L. Minnhagen, *Ark. Fys.* **25**, 203 (1963).
 - [10] K.G. Dyall, I.P. Grant, C.T. Johnson, F.A. Parpia, and E.P. Plummer, *Comput. Phys. Commun.* **55**, 425 (1989).
 - [11] H. Smid and J.E. Hansen, *Phys. Rev. Lett.* **52**, 2138 (1984).
 - [12] Y. Hahn, *Phys. Rev. A* **13**, 1326 (1976).
 - [13] U. Fano, *Phys. Rev.* **124**, 1866 (1961).
 - [14] U. Gelius, *J. Electron Spectrosc. Relat. Phenom.* **5**, 985 (1974).
 - [15] H. Kossmann, B. Krässig, V. Schmidt, and J.E. Hansen, *Phys. Rev. Lett.* **58**, 1620 (1987).
 - [16] M.O. Krause, S.B. Whitfield, C.D. Caldwell, J.-Z. Wu, P. van der Meulen, C.A. de Lange, and R.W.C. Hansen, *J. Electron Spectrosc. Relat. Phenom.* **58**, 79 (1992).
 - [17] V.L. Sukhorukov, B.M. Lagutin, I.D. Petrov, S.V. Lavrentiev, H. Schmoranzner, and K.-H. Schartner, *J. Electron Spectrosc. Relat. Phenom.* **68**, 255 (1994).
 - [18] M. Meyer, E. von Raven, B. Sonntag, and J.E. Hansen, *Phys. Rev. A* **49**, 3685 (1994).